The Journal of Experimental Biology 212, 277-286
Published by The Company of Biologists 2009
doi:10.1242/jeb.021360

Caudal fin shape modulation and control during acceleration, braking and backing maneuvers in bluegill sunfish, *Lepomis macrochirus*

B. E. Flammang* and G. V. Lauder

Museum of Comparative Zoology, Harvard University, 26 Oxford Street, Cambridge, MA 02138, USA

*Author for correspondence (e-mail: bflammang@oeb.harvard.edu)

Accepted 10 November 2008

SUMMARY

Evolutionary patterns of intrinsic caudal musculature in ray-finned fishes show that fine control of the dorsal lobe of the tail evolved first, followed by the ability to control the ventral lobe. This progression of increasing differentiation of musculature suggests specialization of caudal muscle roles. Fine control of fin elements is probably responsible for the range of fin conformations observed during different maneuvering behaviors. Here, we examine the kinematics of the caudal fin and the motor activity of the intrinsic caudal musculature during kick-and-glide, braking and backing maneuvers, and compare these data with our previous work on the function of the caudal fin during steady swimming. Kick-and-glide maneuvers consisted of large-amplitude, rapid lateral excursion of the tail fin, followed by forward movement of the fish with the caudal fin rays adducted to reduce surface area and with the tail held in line with the body. Just before the kick, the flexors dorsalis and ventralis, hypochordal longitudinalis, infracarinalis and supracarinalis showed strong activity. During braking, the dorsal and ventral lobes of the tail moved in opposite directions, forming an 'S'-shape, accompanied by strong activity in the interradialis muscles. During backing up, the ventral lobe initiated a dorsally directed wave along the distal edge of the caudal fin. The relative timing of the intrinsic caudal muscles varied between maneuvers, and their activation was independent of the activity of the red muscle of the axial myomeres in the caudal region. There was no coupling of muscle activity duration and electromyographic burst intensity in the intrinsic caudal muscles during maneuvers, as was observed in previous work on steady swimming. Principal-component analysis produced four components that cumulatively explained 73.6% of the variance and segregated kick-and-glide, braking and backing maneuvers from each other and from steady swimming. The activity patterns of the intrinsic caudal muscles during maneuvering suggest motor control independent from myotomal musculature, and specialization of individual muscles for specific kinematic roles.

Key words: swimming, maneuvering, locomotion, kinematics, electromyography, caudal fin, fish muscle.

INTRODUCTION

Teleost fishes are defined as a monophyletic group by their characteristic caudal skeleton (de Pinna, 1996; Gosline, 1997; Lauder, 1989; Lauder and Liem, 1983; Rosen, 1982). The novel teleost tail design is regarded as evidence for the evolution of distinct locomotory abilities from fishes with heterocercal tail shapes (Gosline, 1997; Lauder, 1989; Lauder and Liem, 1983), and a great deal of research has focused on the supporting skeletal structures and overall movement of the tails of these fishes (Bainbridge, 1963; Grove and Newell, 1936; Lauder, 1989; Lauder, 2000; Lauder and Liem, 1983; Nag, 1967; Nursall, 1958; Nursall, 1963; Webb and Smith, 1980). However, restructuring of the skeletal elements of the tail necessitates coincident changes in muscle, nerve and vascular arrangement (Nag, 1967), although little work has been done to examine the muscular components of the tail, especially in an evolutionary context (Flammang and Lauder, 2008; Gemballa, 2004; Lauder, 1989), and the role that intrinsic tail muscles have in controlling tail shape during a diversity of locomotor behaviors.

Skeletal and muscular structural differences are obvious within the caudal fins of the actinopterygians (ray-finned fishes), and comparisons between gar (*Lepisosteus* spp.), bowfin (*Amia calva*) and bluegill sunfish (*Lepomis macrochirus*) (Fig. 1) (see also Gemballa, 2004; Lauder, 1989) reveal the major evolutionary patterns to caudal fin structure. The transition from heterocercal (externally asymmetrical) to homocercal (externally symmetrical) caudal fin shapes exemplified by these fishes was accomplished through reconstruction of both skeletal and soft-tissue components of the tail. Our dissections corroborate the presence of a single deep intrinsic caudal muscle in gar (Fig. 1), known in the literature as the flexor ventralis (Lauder, 1989) or the musculus flexor profundus (Gemballa, 2004). Additionally, the hypochordal longitudinalis, interradialis and supracarinalis muscles are first apparent in the bowfin (Fig. 1). However, the interradialis muscles in bowfin insert only onto the seven dorsal-most, but not ventral, fin rays. Teleost fishes, such as the bluegill sunfish, are the first fishes to have a flexor dorsalis muscle in the tail and infracarinalis muscles and interradialis muscles between the ventral fin rays (Fig. 1). This phylogenetic pattern shows that a key transition in the evolution of caudal fin structures in ray-finned fishes involves the addition of first more dorsal and then ventral control elements to caudal fin rays. The end result, accomplished with the addition of the infracarinalis, interradialis and supracarinalis muscles in teleost fishes, is hypothesized to be a more maneuverable tail fin that can be formed into different shapes, rather than acting as a rigid propulsive foil (Lauder, 1982; Lauder, 1989).

This evolutionary trend towards specialization of the caudal fin muscles suggests that, as the caudal fin region became differentiated from the axial body myomeres, the increasing division of muscle groups in the tail resulted in progressively finer control of caudal fin elements. However, our previous work on caudal muscle

function during steady swimming showed that there was little functional differentiation among intrinsic tail muscles as speed increased and that tail muscles seemed to be acting simply to stiffen the tail against increased hydrodynamic loads (Flammang and Lauder, 2008). Here, we investigate the range of fin control and shape modulation in bluegill sunfish (*Lepomis macrochirus*) through examination of the kinematics of the caudal fin and activity of the intrinsic caudal musculature during a diversity of unsteady locomotor behaviors: kick-and-glide swimming, braking and backing maneuvers. Analysis of the ability of fish to actively control tail shape with intrinsic musculature during unsteady locomotion is of importance for understanding how the function of the fish tail, often considered in engineering analyses as a rigid plate, is capable of substantial shape change and hence modulation and vectoring of force. Such analyses are also of interest in the light of recent developments in fish robotics and modelling, for which data on fin-ray control could be used to construct more-accurate biomimetic models of fin function (Tangorra et al., 2007; Zhu and Shoele, 2008). We hypothesize that, if intrinsic caudal muscle differentiation in function is present at all, inducing maneuvering locomotor behaviors should generate functional differentiation between muscles that is not seen during steady swimming. We also consider the biological and evolutionary importance of discrete, specialized intrinsic caudal musculature in bony fishes and emphasize the important role of the little-studied intrinsic tail musculature in fish locomotion.

MATERIALS AND METHODS

Fish

The data presented here were collected during the same experiments on steady swimming in bluegill sunfish (*Lepomis macrochirus* Rafinesque) presented by Flammang and Lauder (Flammang and Lauder, 2008). Five fish of similar size (17.4±1.9 cm total length, mean ± s.d.) were used for both electromyographic and kinematic study of maneuvering behaviors. Fish were collected from ponds near Concord, MA, USA under a valid State of Massachusetts (USA) scientific collecting permit and maintained in individual 40 l aquaria at approximately 20°C. Fish were fed three times per week. Fish were placed into the flow tank two days before experiments for acclimation and training and were not fed during this time to ensure a feeding response during the experiment.

Electromyographic protocol

The surgical insertion methods for electrodes used in these experiments were the same as we presented in Flammang and Lauder (Flammang and Lauder, 2008) for the study of steady swimming in the same bluegill sunfish. The comparisons presented below between steady swimming and maneuvering muscle activity patterns thus involve the same fish and the same electrodes. Fish were anaesthetized using tricaine methanesulfonate (MS222) and ventilated during electrode placement, as in previous studies (Flammang and Lauder, 2008; Jayne and Lauder, 1993; Jayne et al., 1996; Tytell and Lauder, 2002). The electrodes were made of 0.05 mm bifilar Teflon-coated steel and were 2 m in length with 0.5 mm of the tips bared of insulation and split apart so as not to be in contact. Subcutaneous implantation of each electrode into muscle was performed using a sterile 26-guage needle.

Electrodes were placed bilaterally in the flexor dorsalis (FD), flexor ventralis (FV), hypochordal longitudinalis (HL), infracarinalis posterior (IC), nine interradialis (IR) muscles, lateralis superficialis (LS), supracarinalis posterior (SC) and the peduncular red myotomal muscle (RED). Fish were allowed to recuperate in the flow tank for at least twice as long as the surgery had lasted before experiments began. Electromyographic (EMG) signals were recorded from 13 muscles at a time for each maneuver and amplified 5000 times through Grass model P511K amplifiers set to filter at high bandpass (100 Hz) and low bandpass (3 kHz), with a 60 Hz notch filter. Digital recordings were captured in Chart 5.4.2 software using an ADInstruments PowerLab/16SP analog-to-digital converter (ADInstruments, Colorado Springs, CO, USA). Following the experiments, fish were euthanized and preserved in formalin, and electrodes were dissected out to verify placement post-mortem.

Kinematic protocol

Experiments were conducted in a 600 l flow tank with a 26 cm by 26 cm by 80 cm working volume, as in previous research (Flammang and Lauder, 2008; Standen and Lauder, 2005; Tytell, 2006). Three synchronized high-speed video cameras (Photron USA, San Diego, CA, USA) were positioned to record simultaneously the fish swimming in the lateral, posterior and ventral views. Kick-and-glide, braking and backing maneuvers were filmed at 250 frames s^{-1} with 1024 by 1024 pixel resolution.

Unsteady swimming behaviors were elicited by altering flow speed and introducing prey or barriers. Kick-and-glide behaviors were exhibited at swimming speeds greater than or equal to 2.0 body lengths per second ($L\,s^{-1}$), and were defined as a single tail beat followed by a period during which the caudal fin was not moved laterally but the fish continued to make forward progress. Braking maneuvers were elicited by turning off the flow in the recirculating flow tank, positioning the fish downstream but facing upstream, and dropping a worm in front of the upstream baffle grate. Fish accelerated towards the prey item and were forced to stop quickly as they approached the end of the swim area. The onset of the braking maneuver was determined to be the time of prey capture, which was visible in the high-speed video recordings. The end of the braking maneuver was determined to be the cessation of forward travel of the fish. To obtain backing sequences, fish were kept facing upstream by introducing flow of about $0.25\,L\,s^{-1}$, and a 1 cm diameter wooden rod was placed 2–3 cm in front of the head of the fish. As the rod was moved downstream slowly, the fish began to swim backwards. A backwards tail beat was defined as 360° of lateral excursion of the ventral tip of the caudal fin, which initiated the backing tail beat.

Data analysis

A trigger-signal synchronized video and EMG recordings, and only the EMG recordings that corresponded with a clear view of the caudal fin in the lateral, posterior and ventral views, were analyzed. The video views were calibrated in three dimensions using direct linear transformation of a custom 20-point calibration frame and digitized using a program written for MATLAB 7 (MathWorks, Natick, MA, USA) by Ty Hedrick (Flammang and Lauder, 2008; Hatze, 1988; Hedrick et al., 2002; Hsieh, 2003; Standen and Lauder, 2005). A total of five points in the caudal region of each fish were digitized: (1) the posterior end of the second fin ray at the tip of the dorsal lobe, (2) the posterior end of the ninth fin ray in the fork of the caudal fin, (3) the posterior end of the fifteenth fin ray at the tip of the ventral lobe, (4) the insertion of the anal fin at the anterior ventral edge of the caudal peduncle and (5) the posterior ventral edge of the caudal peduncle, at the base of the first ventral raylet. Two kinematic variables were used to describe the action of the tail fin, as in Flammang and Lauder (Flammang and Lauder, 2008): mean lateral excursion (cm) and mean tail height (cm) measured in three dimensions. Chart 5.5.5 software (ADInstruments, Colorado Springs, CO, USA) was used to rectify,

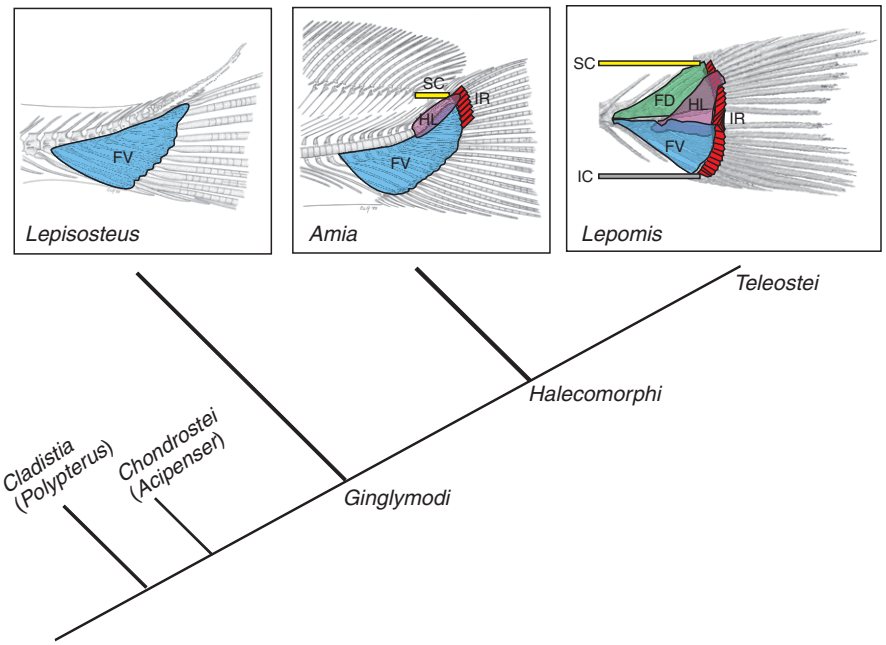

Fig. 1. Cladogram representing phylogenetic relationships between major groups of actinopterygian (ray-finned) fishes. Diagrams of gar (*Lepisosteus*) and bowfin (*Amia*) skeletons are modified from Lauder (Lauder, 1989), with color outlines of intrinsic caudal muscles added. The color coding of the muscles is the same used for the bluegill sunfish (*Lepomis*) in Flammang and Lauder (Flammang and Lauder, 2008) and in Figs 5–7 here. The intrinsic caudal muscles represented are the flexor dorsalis (FD, green), flexor ventralis (FV, blue), hypochordal longitudinalis (HL, purple), infracarinalis (IC, gray), interradialis (IR, red) and supracarinalis (SC, yellow). Note that *Lepisosteus* lacks all intrinsic caudal musculature except for a broad FV, and *Amia* lacks the FD, IC and all ventral IR muscles.

integrate and digitize the onset, duration and intensity of the EMG (defined as the area of the rectified EMG burst) recordings for each maneuver.

RESULTS

Bluegill sunfish are able to modulate the shape of their tail fins into a variety of configurations different than that exhibited during steady swimming ($1.2\,L\,s^{-1}$) (Fig. 2A), depending on the behavior being performed. Braking maneuvers followed acceleration towards prey and were characterized by a rapid flaring of the dorsal and ventral lobes of the caudal fin in opposite directions (Fig. 2B). Backing maneuvers often followed braking maneuvers. Kick maneuvers (Fig. 2C) were characterized by sudden rapid lateral excursion of the caudal fin and were followed by a forward glide ('kick-and-glide') (Fig. 2D).

The sinusoidal mean lateral excursion pattern of the dorsal tip of the caudal fin during steady swimming was not present in the unsteady swimming maneuvers (Fig. 3A). Steady swimming at $1.2\,L\,s^{-1}$ resulted in a lateral excursion from the fish median axis of approximately 1 cm in both the right and left directions (Flammang and Lauder, 2008). During kick-and-glide maneuvers, mean lateral excursion reached 2.5±0.12 cm (mean±s.e.m.) maximum during rapid kicks, but the caudal fin returned to near the median axis (directly behind the fish) during the glide phase (Fig. 3A, red triangles). The duration of an average tail beat during a kick was 0.11±0.01 s. Glides following a kick were sustained for an average of 0.16±0.03 s. During braking maneuvers (Fig. 3A, white diamonds), the dorsal tip of the tail fin traveled an additional mean 1.33±0.3 cm laterally (after 70% of the tail beat) from its position during the last acceleratory stroke towards the prey item. The mean braking time, or the time to come to a complete stop after prey capture, was 0.059±0.008 s. The maximum lateral excursion of the pectoral fins occurred later, 0.081±0.008 s after prey capture. Backing maneuvers (Fig. 3A, green squares) resulted in the least amount of mean lateral excursion, approximately 0.5 cm to either side.

The greatest mean tail height occurred during the rapid kick maneuvers (6.4±0.06 cm) (Fig. 3B, red triangles). During the forward glide following the kick, the caudal fin rays were held close to the lateral midline of the body, creating a mean tail height of 4.5±0.04 cm (red triangles after 70% of the tail beat) (Fig. 3B). The mean tail height for braking maneuvers (Fig. 3B, white diamonds) was similar initially to the mean tail height during gliding (4.7±0.06 cm) and increased by approximately 1 cm when the dorsal and ventral lobes of the tail were fully flared. The backing maneuver mean tail height (5.7±0.08 cm) (Fig. 3B, green squares) remained relatively constant throughout the tail beat and was similar to mean tail height during steady swimming at $1.2\,L\,s^{-1}$ (5.7±0.09 cm) (Fig. 3B, black circles).

The patterns of mean lateral excursion for the tip of the dorsal lobe (circle), fork of the tail (triangle) and tip of the ventral lobe (square) differed among kick and glide, braking and backing maneuvers (Fig. 4). During kick-and-glide maneuvers, the dorsal and ventral lobe and the fork of the tail all moved in unison throughout the tail beat (Fig. 4A). When braking (Fig. 4B), the dorsal and ventral tail tips spread in opposite directions, while the fork of the tail was in line with the median axis of the fish. For backing maneuvers (Fig. 4C), the dorsal and ventral tail tips move together, but the trailing edge of the tail fin is manipulated into a wave-like pattern that passes from the ventral to dorsal tip. As a result, the fork of the tail is moved in the opposite direction to that of the dorsal and ventral tail tips.

Whereas separate intrinsic caudal muscles were active at different times during steady swimming (Fig. 5A), electromyographic recordings of kicks (Fig. 5B) (from 0.4 to 0.5 s) were nearly simultaneous from all muscles. Strong activity in the FD, FV, HL, IC and SC was evident just before the large-amplitude kick. Electromyographic bursts of the IR greater than 10 mV occurred just before the caudal fin rays were adducted, reducing the surface area of the fin (Fig. 5C). As the tail was positioned behind the body during the glide, there was a reduction in the amplitude of electromyographic activity until only the infracarinalis (IC) was active (Fig. 5D).

Braking maneuvers were initiated by an acceleration followed by prey capture (Fig. 6A), where all intrinsic caudal muscles produced strong electromyographic activity. Often fish would glide towards the prey, and at the onset of braking only the supracarinalis

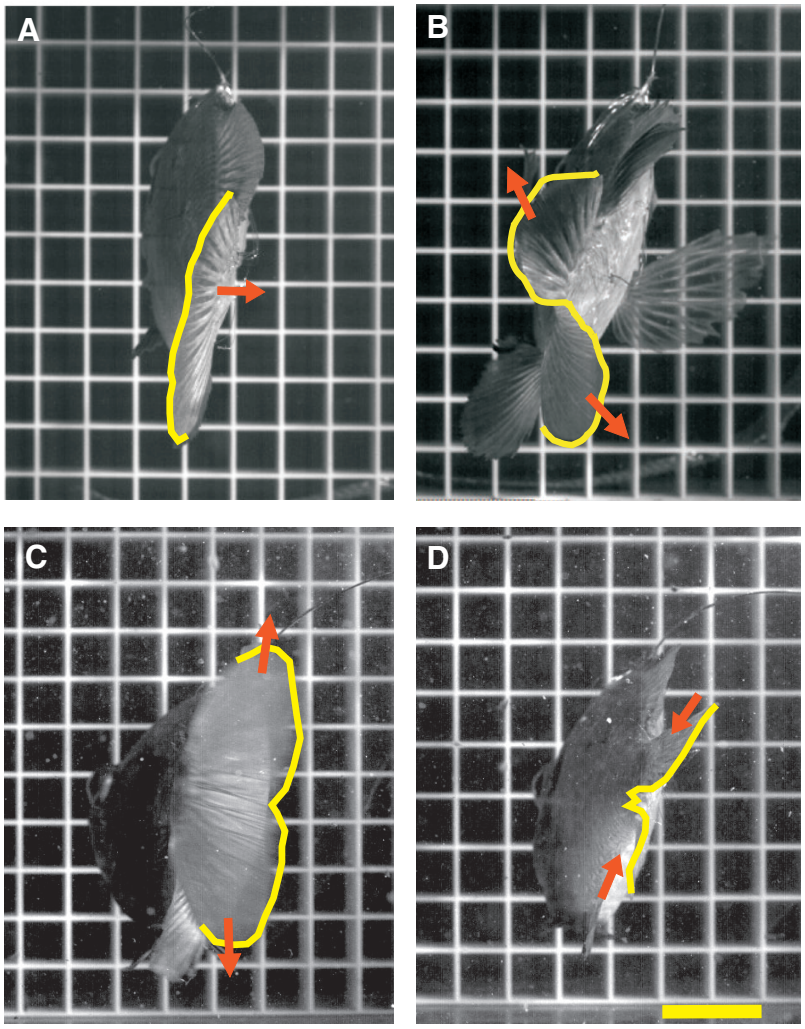

Fig. 2. Representative examples of caudal fin shape modulation in a bluegill sunfish, *Lepomis macrochirus*. Images are frames from posterior-view high-speed video captured during data collection of steady swimming at $1.2\,L\,s^{-1}$ (A), braking (B), and kick (C) and glide (D) maneuvers. Tail outlines closely follow the distal margin of the caudal fin and fin ray position. Arrows indicate the major direction of movement of the dorsal and ventral lobes of the caudal fin. Bar (yellow), 2 cm.

(SC), interradialis (IR) and infracarinalis (IC) muscles were active as the caudal fin rays were spread apart (Fig. 6B). The ventral lobe was moved in the opposite direction from the dorsal lobe (Fig. 6C), giving the tail an 'S'-shaped conformation. Strong IR muscle activity, greater than 10 mV, corresponded with the shape modulation and movement of the caudal fin rays (Fig. 6C). It was not uncommon for fish to switch the direction of the tail curve (Fig. 6D,E), although IR muscle activity was much smaller than during the first 'S'-curve conformation. After forward movement stopped, the fish resumed its normal swimming posture (Fig. 6F).

To swim backwards, fish modulated their caudal fin in a sinusoidal pattern (Fig. 7A–C). Fin motion originated at the ventral tip of the fin, and the wave moved dorsally up the trailing edge of the fin. Just as the wave reached the dorsal tip of the tail fin, the ventral tip was moved in the opposite direction to create a second wave (Fig. 7D,E). Little to no activity was observed in the SC and IC muscles or the red axial myomeres. All other intrinsic caudal muscles were active and the small IR muscles had activity of greater or equal size as the much larger hypochordal longitudinalis (HL), flexor dorsalis (FD) and flexor ventralis (FV) muscles, which was not observed in any other behavior.

Intrinsic caudal muscles did not exhibit the same muscle activity duration, relative onset of muscle activity or EMG burst intensity during kick and glides (Fig. 8, red), braking (Fig. 8, white) and backing (Fig. 8, green) maneuvers as those seen during steady swimming at $1.2\,L\,s^{-1}$ (Fig. 8, black). For all muscles, the onset of muscle activity during kick and glides relative to the activity of the red axial myomere was approximately the same as during steady swimming. The supracarinalis (SC) had the longest relative onset during braking maneuvers. The muscle activity duration of the SC muscle (Fig. 8A) was approximately the same for all maneuvers and steady swimming, but the burst intensity during maneuvers was 2–3 times greater than during steady swimming. The hypochordal longitudinalis (HL) (Fig. 8B) had shorter-duration activity during kick-and-glides and longer-duration activity during backing maneuvers but had the same burst intensity as steady swimming for all maneuvers. The flexor dorsalis (FD) (Fig. 8C) exhibited the same pattern of muscle activity duration between maneuvers as the HL; however, the burst intensity of the FD during braking and backing maneuvers was twice that during kick-and-glide and normal swimming. Muscle activity duration of the ninth interradialis (IR9) (Fig. 8D) muscle was slightly longer for backing maneuvers than all other swimming behaviors; the IR also had the longest relative onset during backing. The EMG burst intensity of IR9 was 2–3 times greater during kick-and-glide and backing maneuvers than during braking and steady swimming. The flexor ventralis (FV) (Fig. 8E) exhibited approximately the same pattern of muscle activity duration and burst intensity as IR9. The infracarinalis (IC) (Fig. 8F) was not active during backing maneuvers at all but had similar activity durations for kick-and-

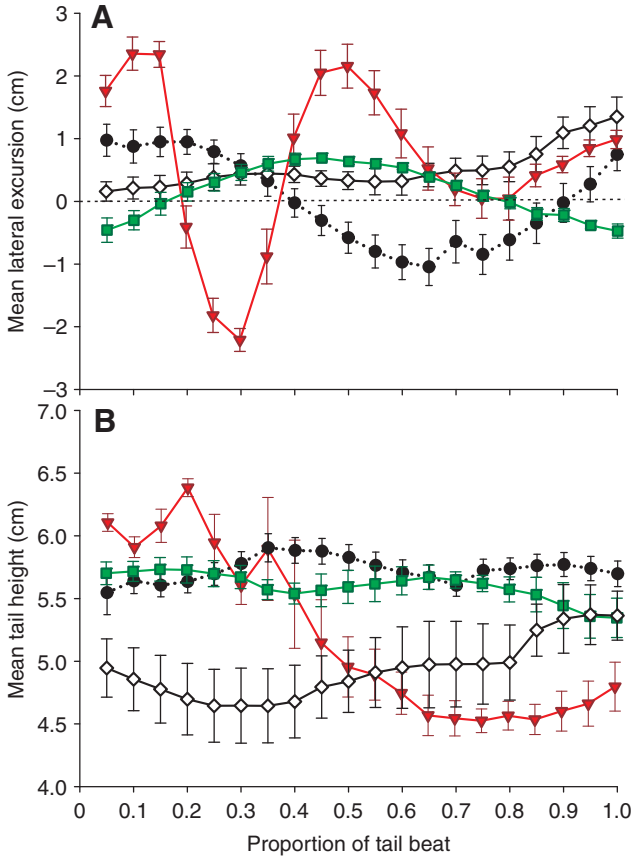

Fig. 3. Plots of mean lateral excursion of the dorsal tip of the tail fin (A) and mean tail height (B) during normal swimming at 1.2 $L\,s^{-1}$ (black circles) (Flammang and Lauder, 2008), kick-and-glide accelerations (red triangles), braking (white diamonds) and backing maneuvers (green squares). All kinematic variables are plotted as the means ± s.e.m.

glide and braking maneuvers as steady swimming. The IC also had twice the EMG burst intensity during kick-and-glides than during braking and steady swimming. The red axial myomere (Fig. 8G) had less than half the muscle activity duration and burst intensity during backing maneuvers as it did during kick-and-glide, braking and steady swimming.

Four factors identified by principal component analysis (PCA) explained 73.6% of the variance in caudal muscle activity duration, relative onset and burst intensity between all three maneuvering behaviors as compared with steady swimming (Table 1; Fig. 9). Principal component 1 (PC1), which characterized the duration of all intrinsic caudal muscles except for the IR and the relative onset of the IR, HL and SC, explained 29.9% of the variance in the EMG recordings. Backing was separated from all other swimming behaviors by PC1. The second principal component (PC2, 19.9% of variance) represented the IR muscle activity duration and relative onset, as well as the duration of the two ventral-most muscles, the FV and IC and separated kick-and-glide maneuvers from braking, backing and steady swimming. 14.3% of variance was explained by PC3, which explained the relative onset and EMG burst intensities of the FD and FV as well as burst intensity of the IR. Principal component 4 (PC4, 9.4% of the variance) represented the inverse relationship between the EMG burst intensity and relative onset of the IC. Braking behaviors were separated from all other swimming behaviors by PC3 and PC4 combined.

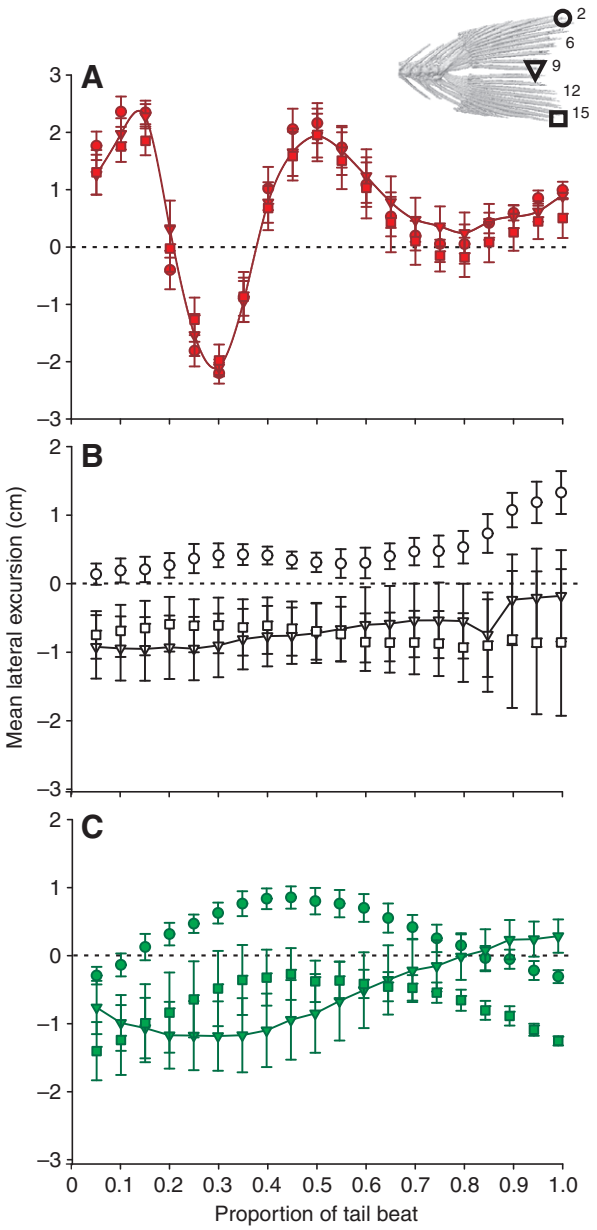

Fig. 4. Plots of mean lateral excursion ± s.e.m. of the dorsal tip (circles), fork (triangles) and ventral tip (squares) of the tail fin during kick-and-glide (A, red), braking (B, white) and backing (C, green) maneuvers. A solid line connects the values for fork of the tail throughout the tail beat to compare against dorsal and ventral tail tip excursion. The dashed zero line indicates the mean direction of travel.

DISCUSSION

While steady swimming in fishes is often described categorically by body undulations of exemplar species (Lauder and Tytell, 2006), maneuvering produces a kinematic repertoire that does not conform to the fin shapes observed in stereotypical steady swimming behaviors. During maneuvers, the motion of the caudal fin often changes irrespective of the motion of the body. To study the shape modulation of tail fins, it is especially important to consider the fin in three dimensions as the fins are not restricted by the normal plane of motion used in steady swimming (Tytell et al., 2008) and to focus on intrinsic tail muscles that cause tail shape modulation. The fins of bony fishes

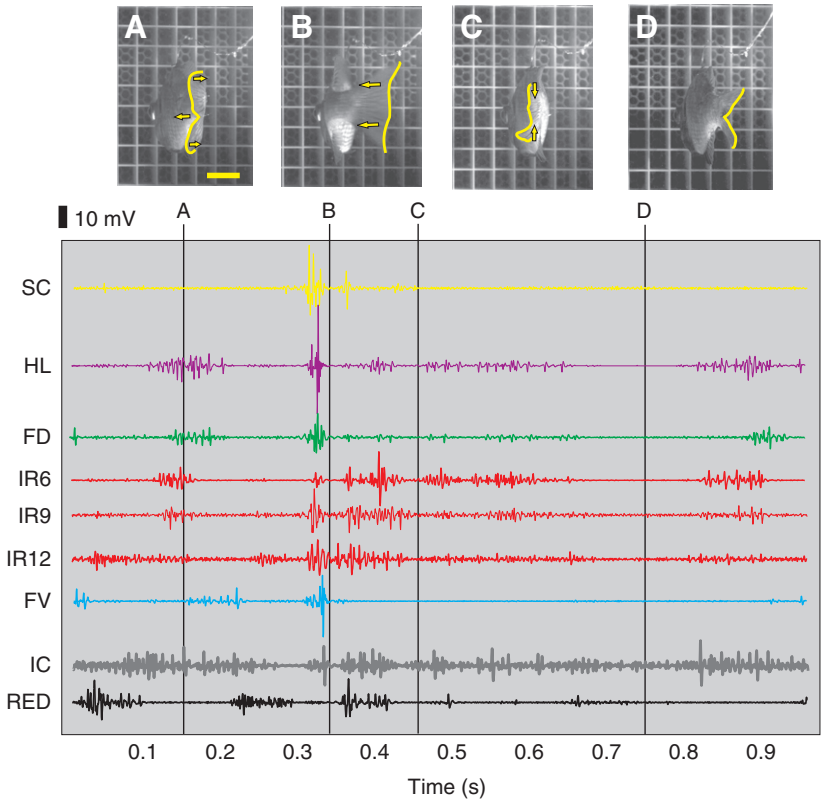

Fig. 5. Kick-and-glide maneuver. Muscle activity is shown for the left supracarinalis (SC), hypochordal longitudinalis (HL), flexor dorsalis (FD), interradialis (IR) designated by its number (6, 9, 12) of dorsally corresponding fin ray, flexor ventralis (FV) and infracarinalis (IC) and right red axial myomere of the caudal peduncle (RED). The colors of electromyographic (EMG) traces are the same as Figs 1, 6 and 7 and as in the Flammang and Lauder study of steady swimming (Flammang and Lauder, 2008). Yellow tail outlines in the images above closely follow the distal margin of the caudal fin and fin ray position. Yellow arrows indicate the major direction of tail lobe movement. Images correspond to a normal tail beat at 2.0 $L\,s^{-1}$ (A), a fast kick (B), beginning of the glide (C) and the end of the glide before a normal tail beat (D). Bar (yellow), 2 cm.

possess an extensive number (25 on each side) of discrete intrinsic tail muscles. These intrinsic caudal muscles are distinct and separate from the axial myotomal body musculature that has been the focus of a great number of studies (Coughlin and Rome, 1996; Goldbogen et al., 2005; Jayne and Lauder, 1994; Jayne and Lauder, 1995; Jayne and Lauder, 1996; Lauder, 1980; Shadwick et al., 1998; Wakeling and Johnston, 1998; Wardle et al., 1995; Westneat et al., 1998). Although intrinsic tail muscles have been described in a number of species (Flammang and Lauder, 2008; Gemballa, 2004; Lauder, 1982; Liem, 1970; Nag, 1967; Videler, 1975; Winterbottom, 1974), there

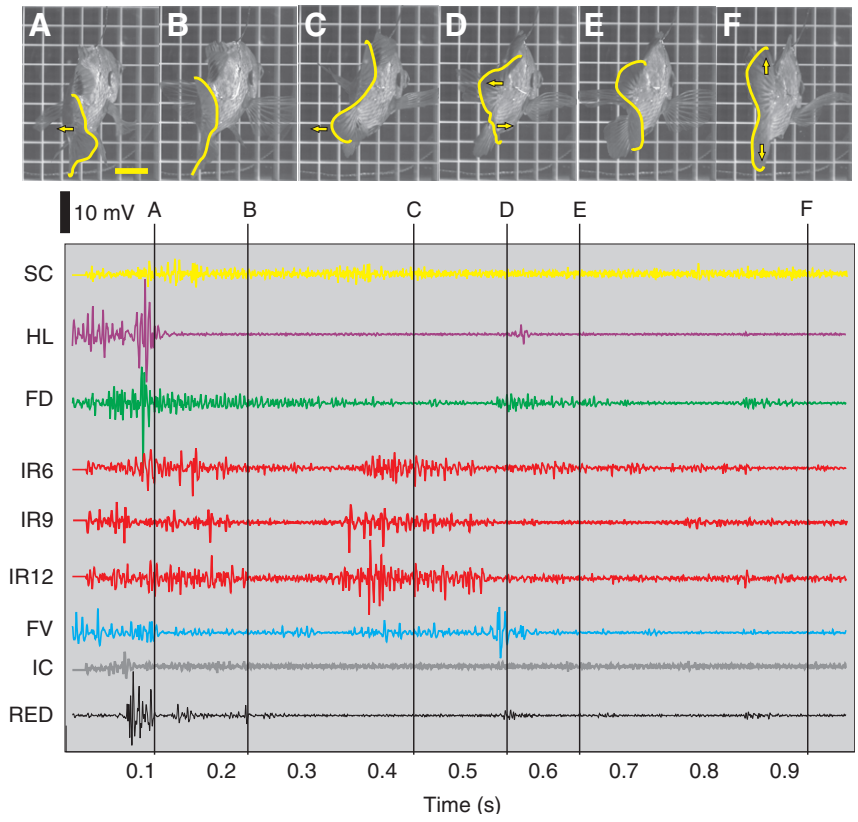

Fig. 6. Acceleration and braking maneuver. Muscle activity is shown for the left supracarinalis (SC), hypochordal longitudinalis (HL), flexor dorsalis (FD), interradialis (IR) designated by its number (6, 9, 12) of dorsally corresponding fin ray, flexor ventralis (FV) and infracarinalis (IC) and right red axial myomere of the caudal peduncle (RED). Yellow tail outlines in the images above closely follow the distal margin of the caudal fin and fin ray position. Yellow arrows indicate the major direction of tail lobe movement. Images are of acceleration towards the prey item (A), flaring and cessation of lateral motion of the caudal fin (B), contralateral movement of the ventral lobe (C), dorsal and ventral lobes moving in the opposite direction (D), 'S'-shaped caudal fin when forward movement of fish stops (E) and preparation to begin swimming again (F). Bar (yellow), 2 cm.

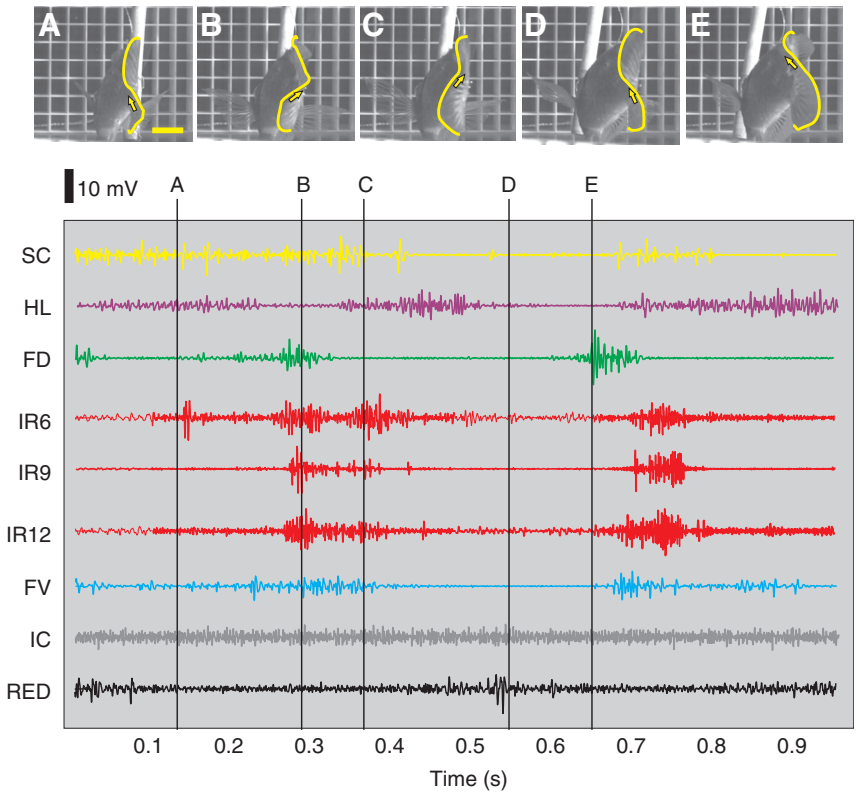

Fig. 7. Backing maneuver. Muscle activity is shown for the left supracarinalis (SC), hypochordal longitudinalis (HL), flexor dorsalis (FD), interradialis (IR) designated by its number (6, 9, 12) of dorsally corresponding fin ray, flexor ventralis (FV) and infracarinalis (IC) and right red axial myomere of the caudal peduncle (RED). Arrows indicate the dorsal progression of the wave along the distal edge of the caudal fin. Tail outlines closely follow the distal margin of the caudal fin and fin ray position. Bar (yellow), 2 cm.

are very few analyses of intrinsic caudal muscle function (Flammang and Lauder, 2008; Lauder, 1982; Lauder, 1989).

In a previous paper (Flammang and Lauder, 2008), we showed that, during steady swimming at speeds approaching 2.0 $L\,s^{-1}$, most of the intrinsic caudal musculature is recruited to stiffen the tail against imposed hydrodynamic loads, with substantial periods of overlap in activity during the tail-beat cycle. Here, we show how a diversity of unsteady locomotor behaviors are accompanied by substantial tail shape changes modulated by an array of different activity patterns of the intrinsic caudal musculature, in contrast to the pattern of intrinsic muscle activity seen during steady swimming.

Comparisons between swimming behaviors

The kinematic patterns and shape modulation of the caudal fin during kick-and-glides, braking and backing maneuvers is markedly different than those observed during steady swimming, as illustrated in Fig. 2. The cause of these diverse fin shapes is the modification of intrinsic caudal muscle activation patterns. Kick-and-glides are performed by

Table 1. Component loadings from principal component analysis of variables analyzed during *Lepomis macrochirus* maneuvering behaviors

	Component loadings			
Variable	PC1	PC2	PC3	PC4
Duration of muscle activity				
Supracarinalis (SC)	0.635	0.466	–0.052	–0.341
Hypochordal longitudinalis (HL)	0.901	–0.152	–0.116	0.179
Flexor dorsalis (FD)	0.737	0.084	–0.260	–0.426
Interradialis 9 (IR9)	0.400	–0.691	0.274	0.040
Flexor ventralis (FV)	0.906	–0.190	0.237	0.078
Infracarinalis (IC)	–0.731	0.525	0.173	–0.188
Relative onset muscle activity				
Supracarinalis	0.623	0.314	–0.080	–0.113
Hypochordal longitudinalis	0.723	0.064	–0.007	–0.408
Flexor dorsalis	0.252	0.210	0.585	0.218
Interradialis 9	0.588	0.567	0.105	0.276
Flexor ventralis	0.062	–0.566	0.540	–0.248
Infracarinalis	–0.035	0.551	0.235	0.603
EMG burst intensity				
Supracarinalis	0.094	0.751	–0.314	0.208
Hypochordal longitudinalis	0.343	0.536	–0.158	–0.352
Flexor dorsalis	0.233	–0.088	–0.844	0.215
Interradialis 9	–0.043	0.703	0.510	–0.013
Flexor ventralis	0.488	0.045	0.712	0.014
Infracarinalis	–0.609	0.310	0.153	–0.613

Principal component 1 (PC1) explained 29.9% of the variance, PC2 19.9%, PC3 14.3% and PC4 9.4%.

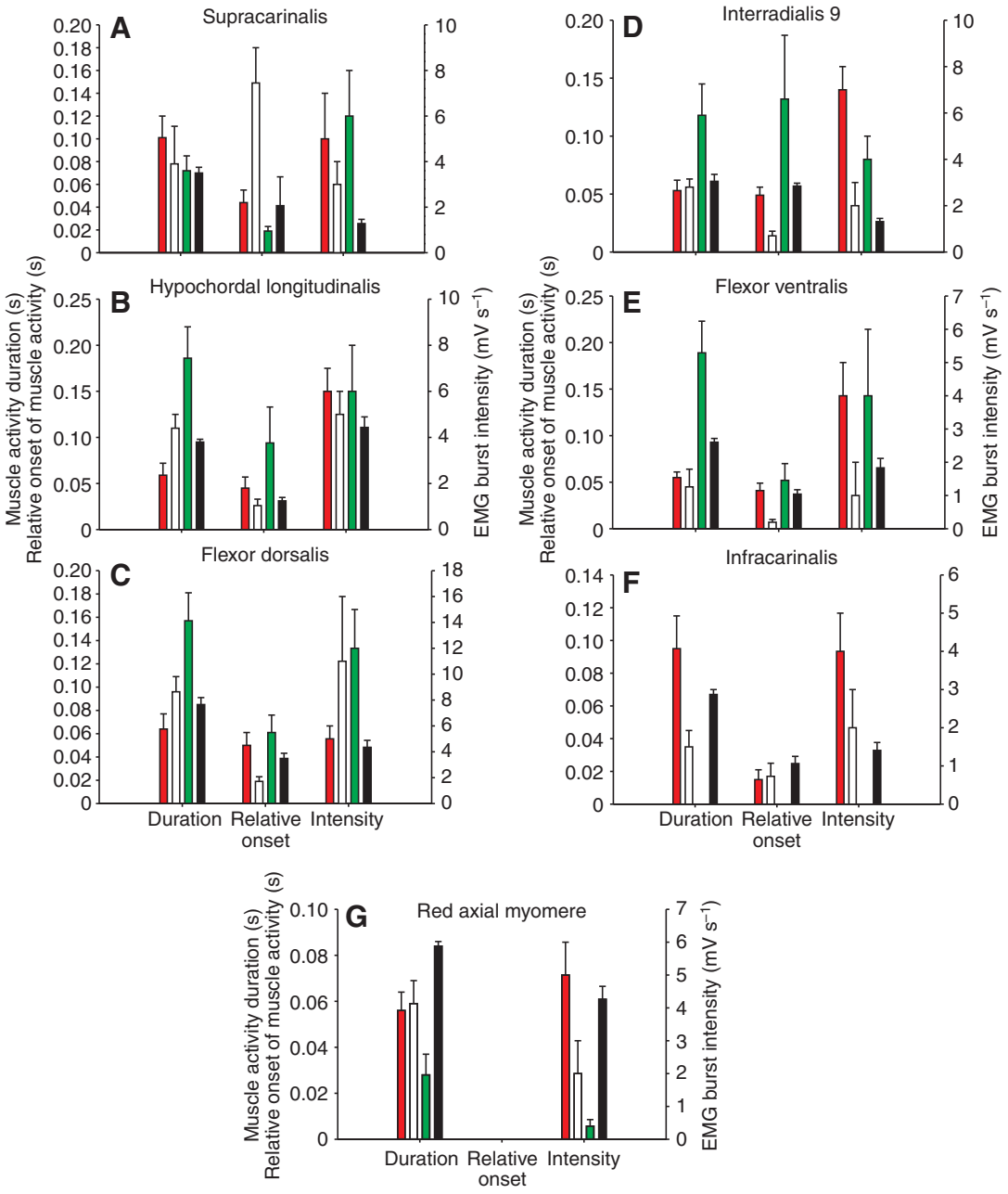

Fig. 8. Histograms of muscle activity duration, onset of muscle activity relative to the red axial myomere and electromyographic (EMG) burst intensity for seven intrinsic tail muscles during kick-and-glide accelerations (red), braking (white), backing maneuver (green) and normal swimming at 1.2 $L\,s^{-1}$ (black) (Flammang and Lauder, 2008). The left-hand *y*-axis is scaled for both muscle activity duration and the relative onset of muscle activity (in seconds), and the right-hand *y*-axis represents the EMG burst intensity (in mV s). Error bars indicate s.e.m. The red axial onset of activity was the reference for other muscle relative onsets.

abduction of the fin rays by the supracarinalis (SC) and infracarinalis (IC) to increase the tail surface area during the kick phase and adduction of the fin rays by the interradialis (IR) to decrease the surface area during the glide phase. Braking was the result of contralateral flaring of the dorsal and ventral lobes of the caudal fin, resulting in increased surface area and, presumably, drag. Breder (Breder, 1926) described a braking behavior with contralateral movement of the caudal fin and dorsal and anal fins, but this behavior was not observed during this study. Backing maneuvers were similar to the reverse of forward steady swimming, with muscle activation originating in the ventral lobe instead of the dorsal lobe.

Although there was an inverse relationship between the duration of muscle activity and EMG burst intensity during steady swimming at increasing speeds (Flammang and Lauder, 2008), the duration and intensity of muscle activity are not coupled during maneuvers. Muscle activity duration remained relatively constant in all muscles during kick-and-glide and braking maneuvers but increased in the three large flexor muscles (flexor dorsalis, FD; flexor ventralis, FV; and hypochordal longitudinalis, HL) and fin ray adductors (IR) during backing maneuvers. These muscles all insert onto the proximal ends of the fin rays and moved the rays in the frontal plane. Thus, backing maneuvers were performed only by slow, lateral

modulation of the fin rays, with little change in fin height. Recruitment of muscles varied by maneuver; the IC was not active at all during backing. Also, the smaller muscles, especially the SC and IR, had EMG burst intensities at least twofold greater during all maneuvers than during steady swimming. Therefore, we conclude that there is more variability in muscle and fiber recruitment during maneuvers in comparison with steady swimming.

Control of caudal fin musculature

Maneuvering is of great ecological importance in fishes, as most species live in complex environments, and control for environmental perturbations requires modulation of fin control surfaces independent of the body (Standen and Lauder, 2005; Walker, 2004; Webb, 1984; Webb, 2004). Fin-controlled maneuvering in teleost fish is performed by precise movements of fan-like segmented fin rays that articulate with the body and support the thin fin membrane (Alben et al., 2007; Arita, 1971; Lauder and Madden, 2007). In the tail, these fin rays are individually controlled by the intrinsic caudal muscles and can move independently of each other and of the body (Flammang and Lauder, 2008; Winterbottom, 1974). Fish caudal fins can also move in a complex three-dimensional manner and alter the direction of fluid flow during swimming (Lauder and Drucker, 2004; Tytell, 2006; Tytell et al., 2008). Fin motion and force generation might compensate in part for the trade-off between stability and maneuverability for a body and allow fishes to both maintain stability as well as maneuver effectively in the aquatic environment (Lauder and Drucker, 2004; Weihs, 2002).

During maneuvers, all intrinsic caudal muscles exhibited relative onset times that were considerably different than those recorded during steady swimming; for example, the relative onset was greatly increased in the supracarinalis during braking and the interradialis during backing (Fig. 8). Activation of these intrinsic tail muscles is thus distinct from activity in the axial myomeres of the body. Previous studies of teleost locomotion focused on axial myomeres have identified a wave-like pattern of muscle activation that passed posteriorly along the fish body, acting as a hybrid oscillator (Fetcho and Svoboda, 1993; Jayne and Lauder, 1995; Lauder, 1980; Long et al., 1994). Generally, the caudal fin has been assumed to be an extension of the axial body during propulsion (Sfakiotakis et al., 1999; Walker, 2004; Webb, 1984). It is known that fishes are also able to spatially restrict active areas of axial myomeres that are specific to localized swimming behaviors (Altringham et al., 1993; Jayne and Lauder, 1995; Thys, 1997). However, more recent work on the kinematics and hydrodynamics of fish fins during steady swimming has shown that the caudal fin is actively modulated irrespective of the action of the body and in concert with the median-dorsal and anal fins (Drucker and Lauder, 2005; Flammang and Lauder, 2008; Tytell, 2006). Specialized and independent activation of the intrinsic caudal muscles irrespective of the axial myomeres, as seen in this paper, suggests separate motor control pathways for intrinsic caudal muscles distinct from myotomal muscle fibers. For example, comparison of electrical activity in the myotomes of the caudal peduncle with intrinsic tail muscles (Figs 5–7) shows clearly that intrinsic caudal muscles can be recruited separately from adjacent myotomal fibers.

Although there are very limited data on the histology of intrinsic caudal musculature in the tail of teleost fishes (Nag, 1972), it appears that each intrinsic muscle might have a mixed red and white fiber population, a pattern distinct from myotomes, where red and white fibers are spatially segregated. These data on caudal muscle histochemistry, if confirmed, coupled with the physiological data presented here on intrinsic muscle activity patterns, suggest that the central spinal circuitry controlling tail musculature might be distinct from that regulating myotomal function. Documenting the fiber types and central neuronal connections of intrinsic tail muscles would certainly be a profitable area of future investigation and could further emphasize the distinct anatomical and functional nature of the tail of teleost fishes, as separate from the main body axis.

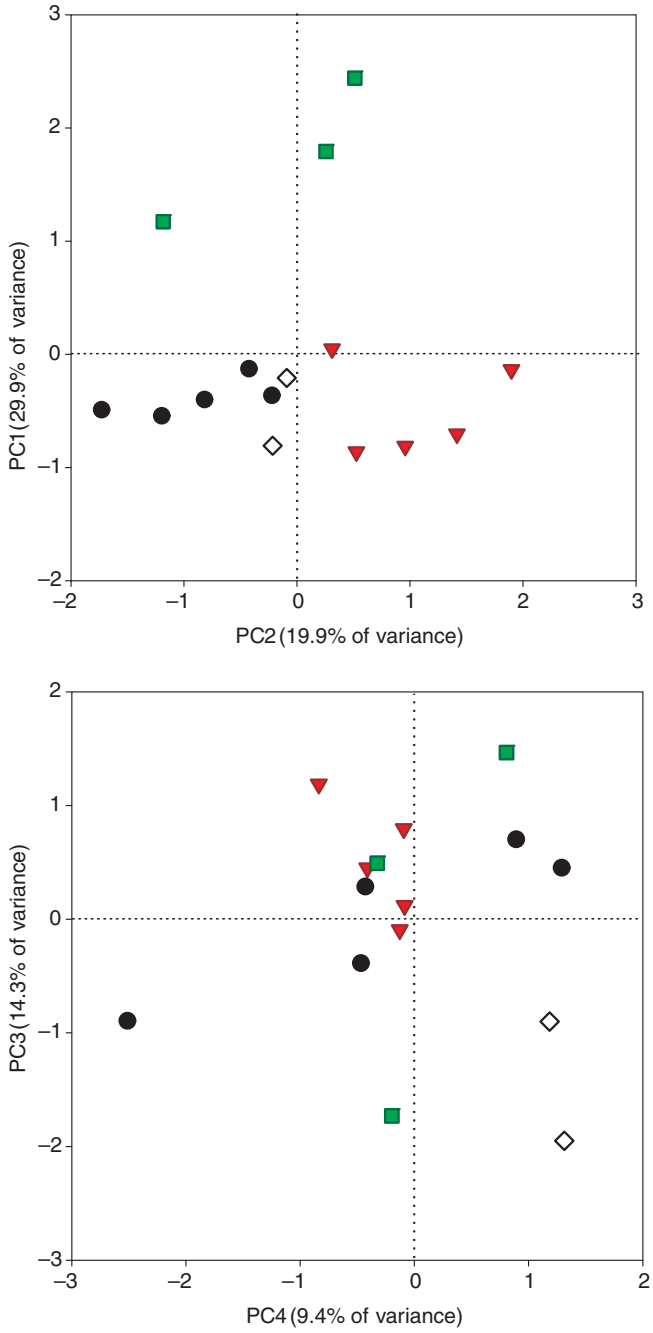

Fig. 9. Principal component analysis of muscle activity duration, relative onset of muscle activity and electromyographic (EMG) burst intensity of all intrinsic caudal muscles except the red axial myomeres during kick-and-glide (red triangles), braking (white diamonds) and backing maneuvers (green squares), and normal swimming at 1.2 $L\,s^{-1}$ (black circles) (Flammang and Lauder, 2008). Each point represents one sequence in which all caudal muscle activity is measured for a given swimming behavior. Further explanation of principal component loadings (Table 1) are given in the text.

The ability of teleost fishes to modulate tail fin shape during maneuvering is a direct consequence of the presence of intrinsic caudal musculature that can be controlled independently of adjacent myotomal fibers. To date, only a few studies have focused on this collection of locomotor muscles, despite their importance in controlling tail function. Caudal skeletal structure is the defining synapomorphy of the teleost fishes (Gemballa, 2004; Gosline, 1997; Lauder, 1982; Lauder, 1989; Lauder and Liem, 1983; Nag, 1967; Nursall, 1963; Winterbottom, 1974), and the coincident changes in muscular and neural arrangement have permitted increasing control and modulation abilities during the course of the evolution of fishes. Future comparative research on the activity of intrinsic tail muscles in basal ray-finned fish taxa such as *Lepisosteus* and *Amia* would allow a broader understanding of the evolution of tail function at the base of the large teleost fish radiation.

We are grateful to S. Kennifer and A. Bonnema for assistance in conducting the experiments, to T. Julius for fish care and maintenance and to the Lauder lab members for insightful discussion. Funding for this research was provided by NSF grant IBN0316675 to G.V.L.

REFERENCES

Alben, S., Madden, P. G. A. and Lauder, G. V. (2007). The mechanics of active fin-shape control in ray-finned fishes. *J. R. Soc. Interface* **4**, 243-256.
Altringham, J. D., Wardle, C. S. and Smith, C. I. (1993). Myotomal muscle function at different locations in the body of a swimming fish. *J. Exp. Biol.* **182**, 191-206.
Arita, G. S. (1971). A re-examination of the functional morphology of the soft-rays in Teleosts. *Copeia* **1971**, 691-697.
Bainbridge, R. (1963). Caudal fin and body movement in the propulsion of some fish. *J. Exp. Biol.* **40**, 23-56.
Breder, C. M. (1926). The locomotion of fishes. *Zoologica* **4**, 159-297.
Coughlin, D. J. and Rome, L. C. (1996). The roles of pink and red muscle in powering steady swimming in Scup, *Stenotomus chrysops*. *Am. Zool.* **36**, 666-677.
de Pinna, M. C. C. (1996). Teleostean monophyly. In *Interrelationships of Fishes* (ed. M. L. J. Stiassny L. R. Parenti and G. D. Johnson), pp. 147-162. San Diego: Academic Press.
Drucker, E. G. and Lauder, G. V. (2005). Locomotor function of the dorsal fin in rainbow trout: kinematic patterns and hydrodynamic forces. *J. Exp. Biol.* **208**, 4479-4494.
Fetcho, J. R. and Svoboda, K. R. (1993). Fictive swimming elicited by electrical stimulation of the midbrain in goldfish. *J. Neurophysiol.* **70**, 765-780.
Flammang, B. E. and Lauder, G. V. (2008). Speed-dependent intrinsic caudal fin muscle recruitment during steady swimming in bluegill sunfish, *Lepomis macrochirus*. *J. Exp. Biol.* **211**, 587-598.
Gemballa, S. (2004). The musculoskeletal system of the caudal fin in the basal Actinopterygii: heterocercy, diphycercy, homocercy. *Zoomorphology* **123**, 15-30.
Goldbogen, J. A., Shadwick, R. E., Fudge, D. S. and Gosline, J. M. (2005). Fast-start muscle dynamics, in the rainbow trout *Oncorhynchus mykiss*: phase relationship of white muscle shortening and body curvature. *J. Exp. Biol.* **208**, 929-938.
Gosline, W. A. (1997). Functional morphology of the caudal skeleton in teleostean fishes. *Ichthyol. Res.* **44**, 137-141.
Grove, A. J. and Newell, G. E. (1936). A mechanical investigation into the effectual action of the caudal fin in some aquatic chordates. *Ann. Mag. Nat. Hist. Ser. 10* **17**, 280-290.
Hatze, H. (1988). High-precision three-dimensional photogrammetric calibration and object space reconstruction using a modified DLT-approach. *J. Biomech.* **21**, 533-538.
Hedrick, T. L., Tobalske, B. W. and Biewener, A. A. (2002). Estimates of circulation and gait change based on a three-dimensional kinematic analysis of flight in cockatiels (*Nymphicus hollandicus*) and ringed turtle-doves (*Streptopelia risoria*). *J. Exp. Biol.* **205**, 1389-1409.
Hsieh, S. T. (2003). Three-dimensional hindlimb kinematics of water running in the plumed basilisk lizard (*Basiliscus plumifrons*). *J. Exp. Biol.* **206**, 4363-4377.
Jayne, B. C. and Lauder, G. V. (1993). Red and white muscle activity and kinematics of the escape response of the bluegill sunfish during swimming. *J. Comp. Physiol. A* **173**, 495-508.
Jayne, B. C. and Lauder, G. V. (1994). How swimming fish use slow and fast muscle fibers: implications for models of vertebrate muscle recruitment. *J. Comp. Physiol. A* **175**, 123-131.
Jayne, B. C. and Lauder, G. V. (1995). Red muscle motor patterns during steady swimming in largemouth bass: effects of speed and correlations with axial kinematics. *J. Exp. Biol.* **198**, 1575-1587.
Jayne, B. C. and Lauder, G. V. (1996). New data on axial locomotion in fishes: how speed affects diversity of kinematics and motor patterns. *Am. Zool.* **36**, 642-655.
Jayne, B. C., Lozada, A. F. and Lauder, G. V. (1996). Function of the dorsal fin in bluegill sunfish: motor patterns during four distinct locomotor behaviors. *J. Morphol.* **228**, 307-326.
Lauder, G. V. (1980). On the relationship of the myotome to the axial skeleton in vertebrate evolution. *Paleobiology* **6**, 51-56.
Lauder, G. V. (1982). Structure and function in the tail of the Pumpkinseed sunfish (*Lepomis gibbosus*). *J. Zool. Lond.* **197**, 483-495.
Lauder, G. V. (1989). Caudal fin locomotion in ray-finned fishes: historical and functional analyses. *Am. Zool.* **29**, 85-102.
Lauder, G. V. (2000). Function of the caudal fin during locomotion in fishes: kinematics, flow visualization, and evolutionary patterns. *Am. Zool.* **40**, 101-122.
Lauder, G. V. and Drucker, E. G. (2004). Morphology and experimental hydrodynamics of fish fin control surfaces. *IEEE J. Oceanic Eng.* **29**, 556-571.
Lauder, G. V. and Liem, K. F. (1983). The evolution and interrelationships of the Actinopterygian fishes. *Bull. Mus. Comp. Zool.* **150**, 95-197.
Lauder, G. V. and Madden, P. G. A. (2007). Fish locomotion: kinematics and hydrodynamics of flexible foil-like fins. *Exp. Fluids* **43**, 641-653.
Lauder, G. V. and Tytell, E. D. (2006). Hydrodynamics of undulatory propulsion. In *Fish Biomechanics* (ed. R. E. Shadwick and G. V. Lauder), pp. 425-468. San Diego: Academic Press.
Liem, K. F. (1970). Comparative functional anatomy of the Nandidae (Pisces: Teleostei). *Fieldiana Zoology* **56**, 7-164.
Long, J. H. J., McHenry, M. J. and Boetticher, N. C. (1994). Undulatory swimming: How traveling waves are produced and modulated in sunfish (*Lepomis gibbosus*). *J. Exp. Biol.* **192**, 129-145.
Nag, A. C. (1967). Functional morphology of the caudal region of certain clupeiform and perciform fishes with reference to the taxonomy. *J. Morphol.* **123**, 529-558.
Nag, A. C. (1972). Ultrastructure and adenosine triphosphate activity of red and white muscle fibers of the caudal region of a fish, *Salmo gairdneri*. *J. Cell Biol.* **55**, 42-57.
Nursall, J. R. (1958). The caudal fin as a hydrofoil. *Evolution* **12**, 116-120.
Nursall, J. R. (1963). The hypurapophysis, an important element of the caudal skeleton. *Copeia* **2**, 458-459.
Rosen, D. E. (1982). Teleostean interrelationships, morphological function and evolutionary inference. *Am. Zool.* **22**, 261-273.
Sfakiotakis, M., Lane, D. M. and Davies, J. B. C. (1999). Review of fish swimming modes for aquatic locomotion. *IEEE J. Oceanic Eng.* **24**, 237-252.
Shadwick, R. E., Steffensen, J. F., Katz, S. L. and Knower, T. (1998). Muscle dynamics in fish during steady swimming. *Am. Zool.* **38**, 755-770.
Standen, E. M. and Lauder, G. V. (2005). Dorsal and anal fin function in bluegill sunfish *Lepomis macrochirus*: three-dimensional kinematics during propulsion and maneuvering. *J. Exp. Biol.* **208**, 2753-2763.
Tangorra, J. L., Davidson, S. N., Hunter, I. W., Madden, P. G. A., Lauder, G. V., Dong, H., Bozkurttas, M. and Mittal, R. (2007). The development of a biologically inspired propulsor for unmanned underwater vehicles. *IEEE J. Oceanic Eng.* **32**, 533-550.
Thys, T. (1997). Spatial variation in epaxial muscle activity during prey strike in largemouth bass (*Micropterus salmoides*). *J. Exp. Biol.* **200**, 3021-3031.
Tytell, E. D. (2006). Median fin function in bluegill sunfish Lepomis macrochirus: streamwise vortex structure during steady swimming. *J. Exp. Biol.* **209**, 1516-1534.
Tytell, E. D. and Lauder, G. V. (2002). The C-start escape response of *Polypterus senegalus*: bilateral muscle activity and variation during stage 1 and 2. *J. Exp. Biol.* **205**, 2591-2603.
Tytell, E. D., Standen, E. M. and Lauder, G. V. (2008). Escaping flatland: three-dimensional kinematics and hydrodynamics of median fins in fishes. *J. Exp. Biol.* **211**, 187-195.
Videler, J. J. (1975). On the interrelationships between morphology and movement in the tail of the cichlid fish *Tilapia nilotica* (L.). *Neth. J. Zool.* **25**, 143-194.
Wakeling, J. M. and Johnston, I. A. (1998). Muscle power output limits fast-start performance in fish. *J. Exp. Biol.* **201**, 1505-1526.
Walker, J. A. (2004). Kinematics and performance of maneuvering control surfaces in teleost fishes. *IEEE J. Oceanic Eng.* **29**, 572-584.
Wardle, C. S. J. J., Videler and J. D., Altringham. (1995). Tuning in to fish swimming waves: body form, swimming mode and muscle function. *J. Exp. Biol.* **198**, 1629-1636.
Webb, P. W. (1984). Body form, locomotion, and foraging in aquatic vertebrates. *Am. Zool.* **24**, 107-120.
Webb, P. W. (2004). Response latencies to postural disturbances in three species of teleostean fishes. *J. Exp. Biol.* **207**, 955-961.
Webb, P. W. and Smith, G. R. (1980). Function of the caudal fin in early fishes. *Copeia* **1980**, 559-562.
Weihs, D. (2002). Stability versus maneuverability in aquatic locomotion. *Integr. Comp. Biol.* **42**, 127-134.
Westneat, M. W., Hale, M. E., McHenry, M. J. and Long, J. H., Jr (1998). Mechanics of the fast-start: muscle function and the role of intramuscular pressure in the escape behavior of *Amia calva* and *Polypterus palmas*. *J. Exp. Biol.* **201**, 3041-3055.
Winterbottom, R. (1974). A descriptive synonymy of the striated muscles of the Teleostei. *Proc. Acad. Nat. Sci. Philadelphia* **125**, 225-317.
Zhu, Q. and Shoele, K. (2008). Propulsion performance of a skeleton-strengthened fin. *J. Exp. Biol.* **211**, 2087-2100.